A Ground-Delay-Based Approach to Reduce Impedance-Based Airspace Complexity

Vishwanath Bulusu*
NASA Ames Research Center, Moffett Field, CA, USA

This paper introduces a ground-delay-based traffic management approach to reduce the impedance-based airspace complexity for a given scenario. This work extends our prior research on developing an impedance-based complexity metric for unmanned aircraft system traffic scenario classification. Impedance-based metric was evaluated for 1045 randomly-generated scenarios. Scenarios with overall impedance above a certain threshold were declared as not feasible. A ground-delay-based approach was developed to be applied to the rest of the scenarios so as to remediate any scenarios with small areas of high impedance on their impedance maps. A sample application is shown for a scenario with sixty flights. The detailed trade-offs between overall accrued system delay, the number of delayed flights, the total number of conflicts and the highest impedance observed as a function of the delay tolerance for each aircraft are provided. Potential applications to Urban Air Mobility traffic scenarios are also discussed.

I. Introduction

Air traffic management approaches that reduce the airspace complexity are needed to support future high density Unmanned Aircraft Systems (UAS) operations in the National Airspace System (NAS). This paper presents a ground-delay-based traffic management approach to reduce the complexity of a given UAS traffic scenario with an associated traffic density or volume.

In conventional aviation, air traffic complexity is evaluated from controller and pilot workload[1–4]. Complexity metrics such as Monitor Alert Parameter (MAP)[5], the maximum number of aircraft an Air Traffic Control (ATC) controller can simultaneously handle, and Dynamic Density (DD)[6, 7], a weighted summation of factors that affect the air traffic complexity, are defined based on an assumption of a structured airspace[8–10]. Air Traffic Management (ATM) approaches such as Airspace Flow Programs (AFP), Ground Delay Programs (GDP), Departure Sequence Program (DSP), Miles-In-Trail (MIT) and Minutes-In Trail (MINIT) are employed to keep the airspace complexity within acceptable limits while mitigating any local complexities to the extent possible. However, due to an evolving ecosystem of novel operations in the NAS, it is not straight-forward whether and to what extent these approaches, developed primarily for highly structured airspace, are suitable. For example, small Unmanned Aircraft Systems (sUAS) and Urban Air Mobility (UAM) operations will occur under a different paradigm where ATC will not necessarily be directly responsible for separation assurance of individual vehicles. As new complexity metrics more suitable for these novel and potentially less structured operations are being explored, it becomes even more necessary to study these ATM approaches in the context of such new metrics.

This paper is part of a continued effort at NASA to understand and model complexity of UAS operations and eventually UAM traffic scenarios. It extends two earlier approaches. Xue [11] introduced a scenario complexity metric based on the number of potential conflicts weighted by the associated conflict resolution cost. Bulusu et.al [12] developed an impedance-based complexity metric which improved upon the first work. The definitions of terms from that work as used in this paper are summarily reproduced in section II.A for reference. An important decision support tool that the impedance-based metric produces is the impedance map of a scenario which shows where the heavily impeded areas are in the airspace. In this paper, a ground-delay-based approach is developed that uses such impedance maps of a scenario, as the basis to evaluate potential ground delay that can reduce the scenario complexity.

First, overall impedance (detailed definition from [12] stated in section II.A) for each of a set of 1045 scenarios, with increasing traffic density, is computed. Assuming there is a certain threshold (global threshold) for this mean global impedance, above which the scenario is not feasible, the set of acceptable scenarios is identified. Next, a subset of these

*Aerospace Research Scientist, Crown Consulting Inc., Aviation Systems Division, NASA Ames Research Center, Moffett Field, CA 94035, USA

scenarios is selected which have areas of high impedance on their impedance maps, i.e. - certain areas on the map have impedance above a local threshold. For these scenarios, a ground-delay-based approach is applied to reduce these high local impedances without increasing the overall impedance. The definitions of overall impedance and impedance maps, and the details of the ground-delay-based approach are presented under section II. Evaluation of particular global and local thresholds is beyond the scope of this paper as the focus is on the ground-delay-based approach and the trade-offs involved. We simply select representative values for these thresholds to show the application of our approach on a sample UAS traffic scenario with 60 flights under section III. The results showed that the ground-delay-based approach successfully reduced the complexity in the airspace. It was also found that the effectiveness of the approach depends on the acceptable delay tolerance for the flights. In the same section, potential application to UAM traffic scenarios is also discussed.

II. Methodology

For this study, the focus is on developing a ground-delay-based approach for operations in a two dimensional horizontal portion of airspace that has no constraints such as controlled airspace, temporary flight restrictions, geo-fences or terrain. In the next two sections the test scenarios and the evaluation of the impedance metric are summarized in detail. Then the ground-delay-based approach is described followed by a list of assumptions for the sample application.

A. The Impedance Metric

The relevant information about the impedance metric from [12] is summarized here. The reader is referred to that full paper for detailed evaluation of the metric. When the number of conflicts are high, a scenario is expected to be complex. However, it may not necessarily be so if those conflicts are isolated. The pattern of traffic flow also contributes to the complexity of the scenario. For example, if the aircraft begin to impede the conflict resolutions of others in the airspace, that leads to high complexity. The impedance metric accounts for both the number of conflicts and the free space available around aircraft in conflict.

To evaluate the complexity of a scenario, first two aircraft are assumed to be in conflict at a given time if they are within a distance $h_{sep} = k.D_{wc}$, of each other, where k is a multiplication factor (≥ 1) and D_{wc} is the well-clear distance (arbitrarily chosen at 50 feet or 15.24 meters for demonstrating the evaluation of the metric). h_{sep} is referred to as *Conflict Distance*. This parameterization was used to calibrate the Impedance evaluation to the region of influence of the conflict resolution method that would have been used in an actual traffic simulation.

Let R be the pre-defined region of interest in two-dimensional Euclidean space, i.e. R $\subset \mathbb{R}^2$. Grid the region into square cells C_{xy} with a side length l, where x is the row number and y is the column number. At each time instant t_i, there is a colored grid/map produced, called the *Impedance Map* I_{t_i} =[I_{xy,t_i}], where the color of a cell indicates its impedance $I_{xy,t_i} \in [0, 1]$, which is basically the proportion of surrounding cells occupied by other aircraft over the next dt seconds. Now, to get a single snapshot of the region, the time slices are collapsed over the entire period of the scenario. This produces the *Impedance Map of the Scenario* I_{xy}. An example is shown in Fig. 1. This can be done by either taking the time mean or a percentile value of each cell's impedance. To understand the severity of impedance in each cell over the entire scenario, the p^{th} percentile value of $I_{xy,t}$ is used to collapse the graphs in time. Finally, to get a single impedance number for the whole scenario, both the space and time dimensions need to be collapsed. To do this, compute the percentage of cells in the time-collapsed map with $I_{xy} \geq P$, where P is the chosen local impedance threshold. This gives *I, the Impedance for the entire scenario*, alternatively referred to as the overall impedance of the scenario.

For example, choosing the 99^{th} percentile value for time collapse and P = 20% for an impedance threshold, results in an impedance value of 0.1 for a scenario. This can be interpreted as 0.1 or 10% of the region has conflicts that are impeded by nearby aircraft in at least one-fifth (20%) of the vicinity, for 1% of the time. In other words, conflicts in almost one-tenth of the region are impeded in the scenario.

The metric computation used three parameters: the conflict distance parameter, k, the time window parameter, dt, and the local impedance threshold, P. After tuning the parameters, the best correlation between impedance-based complexity and ground truth, was found with k = 1.5 (conflict distance of 75 feet), dt = $9sec$ and P = 0.1 for the chosen set of scenarios and conflict resolution method. These parameters are used for our study in this paper.

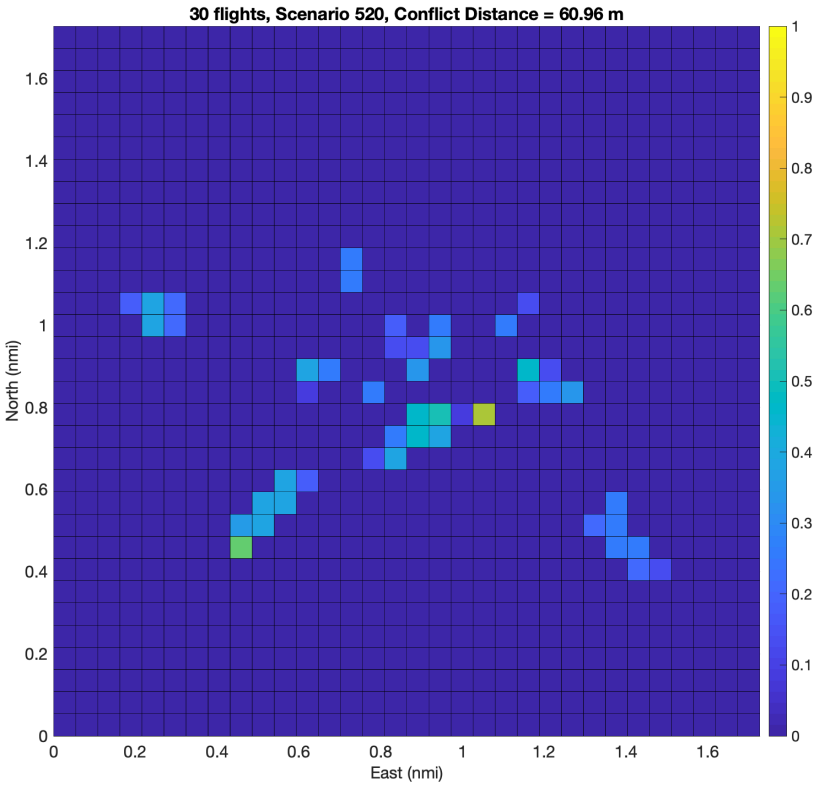

Fig. 1 The Impedance Map of the Sample Scenario with 30 flights at conflict distance, $h_{sep} = 60.96m$, for a time window, dt = 5 sec

B. Test Scenarios

The test scenarios from [11] and [12] are used. 1045 random scenarios with number of flights varying between 5 and 100 (or in density from 3 to 60 vehicles/nmi^2) were generated and evaluated in the Fe^3 [13] simulator to estimate the actual trajectories and total maneuvers if these were actually flown. From 5 to 50, 20 scenarios were generated at each level of density and from 52 to 100, 5 scenarios were generated at every alternate level of density. Several criteria were used to ensure high traffic intensity and comparability in scenarios: First, a 1.3x1.3 nautical mile region is defined (shown as the red box in Fig. 2), where all flights are required to go through with origin and destination being outside of the region; Second, maximum one turning point is allowed en route in a flight plan; Third, all flights are set to depart within a five-minute window; Lastly, the target ground speeds of all flights are in the range of 5 meter per second and 20 meter per second (10 knots to 40 knots approximately). Fig. 2 shows a sample scenario with 30 vehicles, where circle, cross, diamond markers represent origins, destinations, and mid-points respectively.

Using these simulation generated measurements as the ground truth for the scenario complexity, the Impedance (I) metric was evaluated for these scenarios and compared using statistical methods to the ground truth. Their respective impedance maps were also generated. The best correlation with ground truth was observed at a conflict distance of 75 feet, with a time window of 9 sec and a local impedance threshold of 10%. These terms are used as defined in [12] and summarized in section II.A.

C. The Ground-Delay-Based Approach

First step is to identify scenarios where this approach will be employed. To do this, the impedance for all the 1045 scenarios are plotted. These are the single space and time collapsed numbers. A least-squares fit is then generated. This curve is then thresholded with a global impedance threshold. We chose a value of 0.05 for the global threshold. This is

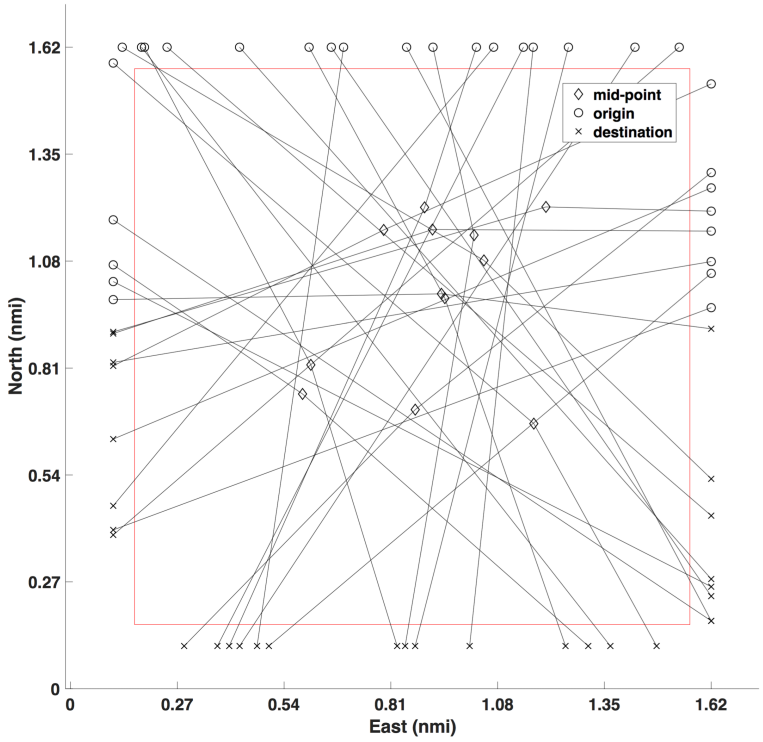

Fig. 2 A sample scenario with 30 flights

shown in Fig. 3. All scenarios with overall impedance above this number are considered not feasible and will not be approved. We note again that this number only says that scenarios with over 5% of the region having highly impeded conflicts are considered too complex. How impeded the particular conflicts are in a scenario that can be approved will matter for our ground-delay-based approach as explained next.

For scenarios under this threshold, their impedance maps are used to identify regions of high impedance (hot spots). An operator can chose how to define the high impedance regions. A local impedance of $P = 0.6$ is chosen to identify high impedance regions in the sample application. Now, given a feasible scenario, the goal of the ground-delay-based approach is to reduce the local impedances exceeding the high threshold, by applying a ground delay up to the given maximum delay tolerance level for the flights in the scenario, while also keeping the overall impedance of the scenario low (under the global threshold). Let this delay tolerance be D_{tol}.

The ground-delay-based algorithm works as follows: For a given scenario, first identify all the flights that pass through hot spots as defined for the scenario. Starting with the earliest flight, for each flight, delay its start by t_{del} sec and recompute the impedance map of the scenario. t_{del} is varied from 1 sec to D_{tol} sec. The delay which produce the maximum reduction in the highest impedance observed in the impedance map of the scenario is kept for that particular flight. This is repeated over all the flights until either all potential delay combinations have been tested or a combination where the highest impedance observed on the map is below the chosen local threshold is found. This produces the new scenario with some flights delayed to reduce the complexity in the airspace. Results for application of this approach to a sample scenario with 60 flights are given.

D. Assumptions

In addition to scenario assumptions stated earlier, the chosen values of different parameters are listed below:

- The cell edge length l = 100 m (0.054 nmi)
- For each scenario, impedance is computed using h_{sep} = 22.86 m, for a time window, dt = 9 sec and local impedance threshold, P = 0.1.
- Three cases of delay tolerance D_{tol} are considered: 9, 18 and 27 seconds. These are multiples of the time window.

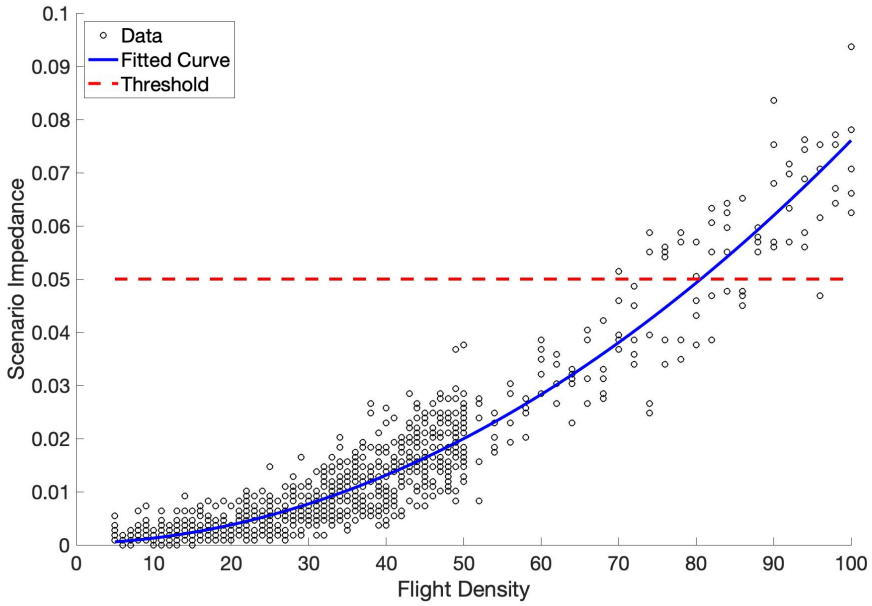

Fig. 3 Impedance for 1045 scenarios with increasing traffic density, $h_{sep} = 22.86m$, for a time window, dt = 9 sec and local impedance threshold, P = 0.1

- t_{del} is varied in 3 second increments. For example, for the 9 second delay tolerance case, a delay of 3, 6 and then 9 sec is tested for each highly impeded flight.
- Since this study focuses on scenario's intrinsic complexity, uncertainties on winds, communications, navigation, and surveillance are not included in the simulations.

For each case of delay tolerance, four values were computed: the total system delay (sum of delays for each delayed flight in a scenario), the total number of delayed aircraft, the total number of conflicts and the highest impedance observed on the map (with and without ground delay). The total number of conflicts, as identified in [11] was another complexity metric used for comparison in earlier work.

III. Results

For the sample application to a scenario with 60 flights, Fig. 4 shows the total system delay and the number of delayed flights while Fig. 5 shows the change in complexity. It was observed that as the delay tolerance increased, the overall system delay increased. However, the number of additional flights delayed didn't increase as much. When tolerance was 9 sec, 4 flights were delayed. When it was increased to 18 sec and 27 sec, only an additional flight was delayed at each step. At the same time, the total number of conflicts decreased with increased tolerance. The highest impedance observed followed a similar trend except it seemed to slightly increase when the tolerance was increased from 18 sec to 27 sec. The increase may not necessarily be bad for the reasons described next.

To get a visual understanding of what is happening, the final impedance maps were generated for each delay tolerance along with the original map without any delay. These are shown in Fig. 6. There were two grid cells with impedance above 0.6 in the original map (the bright yellow and bright green cells near the center) with no delay. As the delay tolerance is increased till 18 sec, the cells become darker near that region and some cells further away become slightly brighter. This seems to show that the reduction in the impedance in the hot spots is also partly achieved by its dispersion in the area around. This is analogous to typical air traffic management strategies in that the airspace is used as a resource to spread out conflicts in space and time and make them less severe. As the tolerance is increased further to 27 sec, overall impedance reduced and dispersed further but the highest impedance went up slightly. This might be an artifact of the traffic pattern in this scenario. It seems to suggest that delaying certain flights too much might push them into more impeded conflicts with later aircraft in the airspace. This therefore suggests that analyzing higher delay tolerances

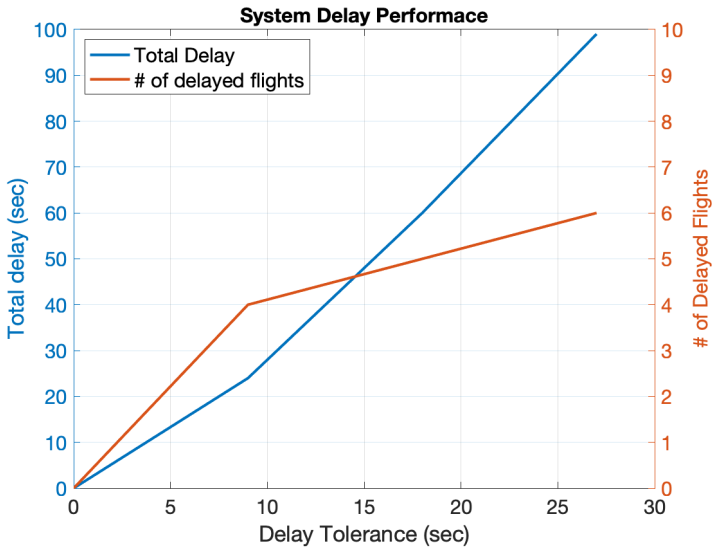

Fig. 4 The total system delay and the number of delayed flights as a function of delay tolerance.

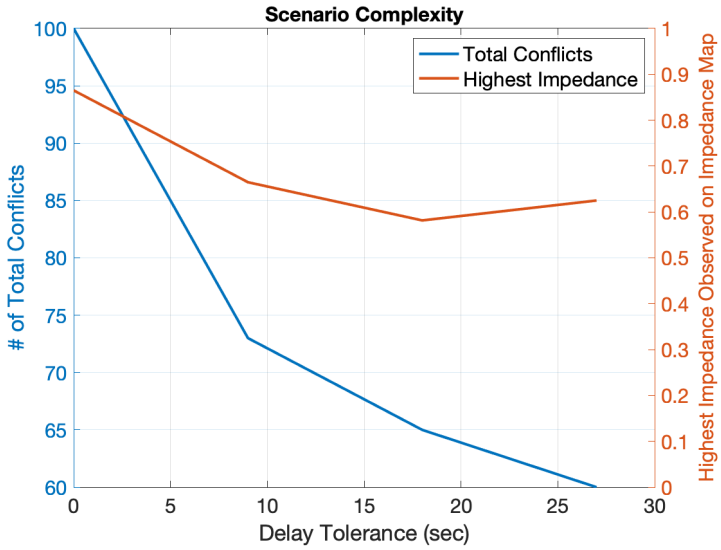

Fig. 5 The number of total conflicts and the highest impedance observed on the impedance map as a function of the delay tolerance.

and with smaller increments might be a good strategy for such scenarios as it enables finer delay adjustments.

A. Applications

In conventional manned aviation, GDP are implemented to control air traffic volume to airports where the projected traffic demand is expected to exceed the airport's acceptance rate for a long period of time. Aircraft are delayed at their departure airport in order to manage demand and capacity at their arrival airport. Delay on ground is preferable to delay in air as it saves fuel. This becomes even more critical for UAS operations fueled by batteries. Hence, the approach developed in this paper builds on that insight to reduce complexity in UAS operations. The approach also borrows insights from AFP in that it calculates ground delays to mitigate an en-route airspace constraint. The difference however is that the ground delay here intends to reduce local airspace impedance rather than meeting an en route flow-rate constraint.

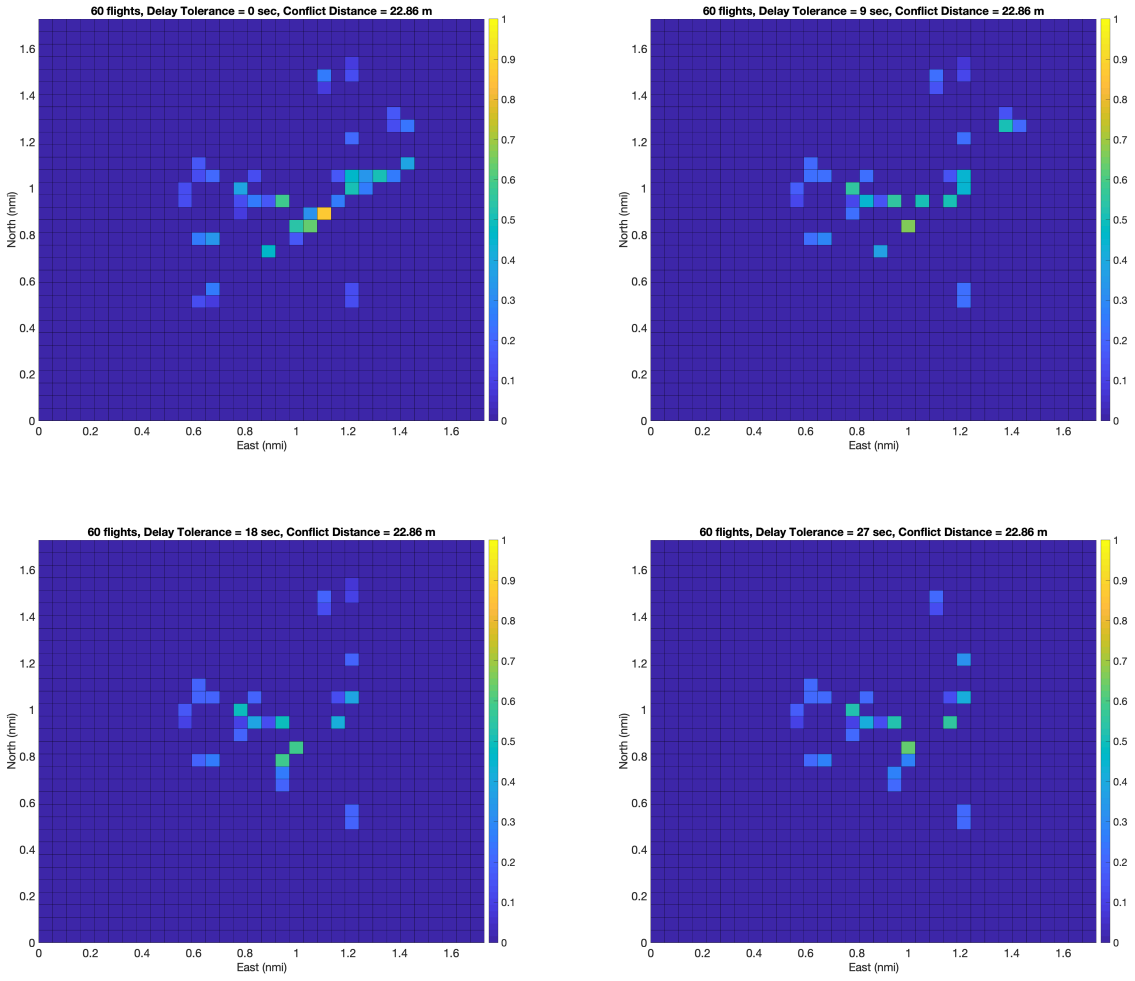

Fig. 6 Impedance maps with varying delay tolerance.

For low-altitude UAS traffic, this can be applied to regions with high operational demand to identify and postpone/reject flight requests that could potentially lead to excessive congestion or safety concerns in a given traffic scenario. The afore-mentioned trade-offs could further enable distributing delays over flights dependent on what factor is valued more in a particular situation, such as system delay vs individual flight delays.

Although, the sample scenarios used have direct origin to destination traffic, the impedance metric computation and the ground-delay-based approach based on it are generalizable to non-direct traffic. They can be applied to traffic around airspace constraints. Hence, this approach can also be extended to UAM traffic scenarios. For example, Bulusu et.al. [14] used trip data for over 300,000 commute trips in the San Francisco Bay Area to locate vertiports so as to maximize the travel time savings for those commuters if they chose to use UAM. One of their optimal combinations (see Fig. 7) with 26 vertiports on the west and 30 on the east of the bay benefited almost one-third of the sample traffic. In a typical UAM scenario for these cross-bay commuters, traffic will be generated from the combination of origin and destination vertiports. Every time new flights are filed in the system, the impedance maps can be generated to identify the hot spots and then the ground-delay-based approach can be applied as needed. Over time, this will provide insights into identifying particular vertiports and spatial and temporal traffic patterns that tend to affect the airspace complexity most. This will lead to systemic improvements in UAM traffic and help balance demand and capacity.

*Underlying map data is © OpenStreetMap contributors. https://www.openstreetmap.org/copyright

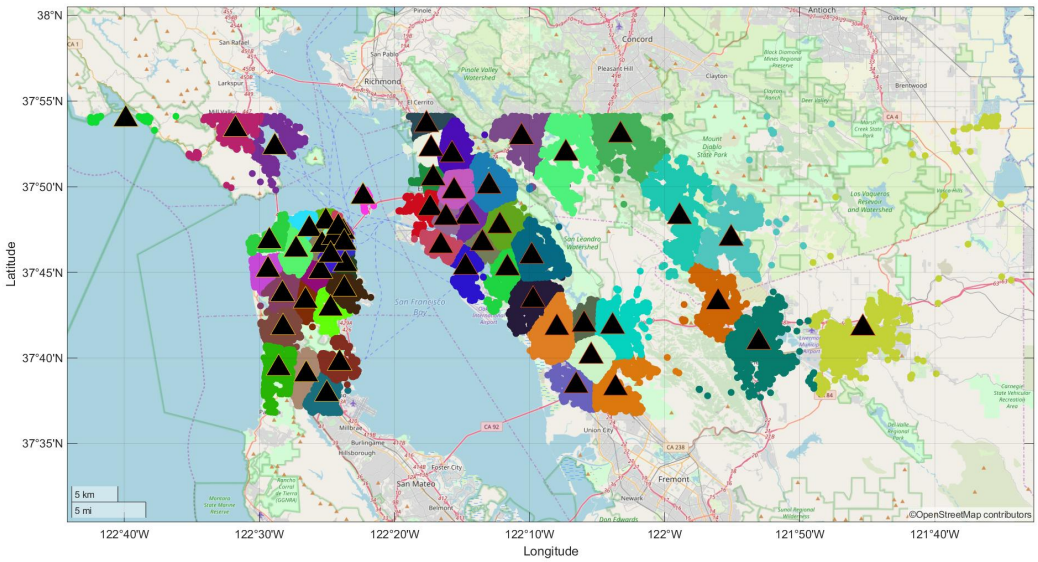

Fig. 7 One of the optimal vertiport combination identified in [14] for the San Francisco Bay Area. The black triangles represent the vertiport locations.*

IV. Conclusions

This paper introduced a ground-delay-based ATM approach to reduce the impedance based airspace complexity for a given scenario. It extends our prior research on developing an impedance based complexity metric for UAS traffic scenario classification. Impedance based metric was evaluated for 1045 randomly-generated scenarios. Scenarios with overall impedance above a certain threshold were declared as not feasible. A ground-delay-based approach was developed to be applied to the rest of the scenarios so as to remediate any scenarios with small areas of high impedance on their impedance maps.

The ground-delay-based approach sought to reduce highest impedances observed on the impedance map of the scenario by delaying the start time of the flights which were supposed to fly through the hot spots. The approach was analyzed at varying levels of delay tolerance for the flights. A sample application was shown for a scenario with sixty flights. The results presented in this paper showed that as the delay tolerance was increased, the system delay and number of flights delayed also increased. At the same time, the scenario complexity decreased as evidenced by the reduction in the total number of conflicts and the highest impedance observed in the maps after adding delays. The particular trend observed suggested that a delay tolerance of 18 sec performed optimally for the chosen sample scenario.

Applications of the approach were also discussed including extension to potential UAM traffic scenarios. This work develops our suite of complexity analysis and traffic management tools further for managing traffic from novel entrants to the airspace. Another strategy to explore would be a change in flight trajectory spatially for flights through the hot spots or a combination of both spatial and temporal trajectory changes.

Acknowledgments

This work was funded by the UAM sub-project at NASA Ames Research Center. I thank Dr. Min Xue, Dr. Banavar Sridhar and Dr. Husni Idris for providing valuable insights and guidance.

References

[1] Majumdar, A., Ochieng, W., and Polak, J., "Estimation of European airspace capacity from a model of controller workload," *Journal of Navigation*, Vol. 55, No. 03, 2002, pp. 381–403.

[2] Majumdar, A., Ochieng, W. Y., Bentham, J., and Richards, M., "En-route sector capacity estimation methodologies: An

international survey," *Journal of Air Transport Management*, Vol. 11, No. 6, 2005, pp. 375–387.

[3] Klein, A., Cook, L., Wood, B., and Simenauer, D., "Airspace capacity estimation using flows and weather-impacted traffic index," *2008 Integrated Communications, Navigation and Surveillance Conference*, IEEE, 2008, pp. 1–12.

[4] Krozel, J., Mitchell, J., Polishchuk, V., and Prete, J., "Airspace capacity estimation with convective weather constraints," *AIAA Guidance, Navigation, and Control Conference*, 2007.

[5] Welch, J. D., Andrews, J. W., Martin, B. D., and Sridhar, B., "Macroscopic workload model for estimating en route sector capacity," *Proc. of 7th USA/Europe ATM Research and Development Seminar, Barcelona, Spain*, 2007, p. 138.

[6] Laudeman, I., Shelden, S., Branstrom, R., and Brasil, C., "Dynamic density: An air traffic management metric (NASA/TM-1998-112226)," *Moffett Field, CA: NASA Ames*, 1998.

[7] Sridhar, B., Sheth, K. S., and Grabbe, S., "Airspace complexity and its application in air traffic management," *2nd USA/Europe Air Traffic Management R&D Seminar*, 1998, pp. 1–6.

[8] Mogford, R. H., Guttman, J., Morrow, S., and Kopardekar, P., "The Complexity Construct in Air Traffic Control: A Review and Synthesis of the Literature." Tech. rep., DTIC Document, 1995.

[9] Kopardekar, P., "Dynamic density: A review of proposed variables," *FAA internal document. overall conclusions and recommendations, Federal Aviation Administration*, 2000.

[10] Kopardekar, P. H., Schwartz, A., Magyarits, S., and Rhodes, J., "Airspace complexity measurement: An air traffic control simulation analysis," *International Journal of Industrial Engineering: Theory, Applications and Practice*, Vol. 16, No. 1, 2009, pp. 61–70.

[11] Xue, M., and Do, M., "Scenario Complexity for Unmanned Aircraft System Traffic," *AIAA Aviation 2019 Forum*, 2019.

[12] Bulusu, V., Sridhar, B., and Xue, M., "An Impedance-Based Complexity Metric for Unmanned Aircraft System Traffic Scenario Classification," *AIAA AVIATION 2020 FORUM*, 2020.

[13] Xue, M., Rios, J., Silva, J., Ishihara, A., and Zhu, Z., "Fe3: An Evaluation Tool for Low-Altitude Air Traffic Operations," *AIAA Aviation Forum*, Atlanta, GA., 2018.

[14] Bulusu, V., Burak Onat, E., Sengupta, R., Yedavalli, P., and Macfarlane, J., "A Traffic Demand Analysis Method for Urban Air Mobility," *IEEE Transactions on Intelligent Transportation Systems - Special Issue on UTM*, 2021.